BI-TP 92/39

INTERQUARK FORCES*

Edwin Laermann

Fakultät für Physik, Universität Bielefeld, D-4800 Bielefeld 1, Germany

ABSTRACT

Strong confining forces between quarks are discussed. The present experimental situation is briefly summarized and compared with theoretical approaches. In particular, results of lattice simulations are reviewed in some detail.

---

* Talk given at the workshop on "QCD – 20 Years Later", Aachen (Germany), June 9-13, 1992.

BI-TP 92/39
October 1992

INTERQUARK FORCES

E. LAERMANN
Fakultät für Physik, Universität Bielefeld
D-4800 Bielefeld, Germany

ABSTRACT

Strong confining forces between quarks are discussed. The present experimental situation is briefly summarized and compared with theoretical approaches. In particular, results of lattice simulations are reviewed in some detail.

1. Introduction

Interquark forces are a central problem in QCD which even 20 years later is not yet solved to a completely satisfactory degree. While at small quark distances the theory is being exploited perturbatively with great success, working out the long-range part of quark interactions poses problems and difficulties which are related to the necessity for a non-perturbative treatment. Since the discovery of the J/ψ, heavy quarkonia have been a unique place to study the long-distance behavior of QCD while, at the same, they allow a link to the perturbative regime.

The distinctive property of heavy quarkonia is their weight. For quarks which are heavy enough a non-relativistic approach can be justified. The average quark velocities in $1S$ $c\bar{c}$ and $b\bar{b}$ quarkonium states are small, $\langle v^2/c^2 \rangle = 0.25$ and 0.08 respectively. Thus certainly for bottonium a non-relativistic treatment seems to be appropriate, whereas this might be debatable for charmonium. The main advantage of the non-relativistic treatment lies in the possibility to apply techniques for bound state problems which are well known from atomic physics. In particular, one can formulate the problem in terms of a Schrödinger equation which may then be solved to obtain the spectrum as well as the bound state wave functions. Moreover, the non-relativistic approach allows a simple formulation of the confinement hypothesis in terms of a potential which grows when the distance between heavy quarks is increased.

The mass of heavy quarkonia also permits to use perturbation theory in certain instances. According to general reasoning, the annihilation of a heavy quark-antiquark pair takes place at distances of the order of the inverse heavy quark mass. Thus, such a process is dominated by the dynamics at short distances and can be treated perturbatively. In the well-known example of quarkonium decays into hadrons the branching ratios have been successfully calculated via quark annihilation into gluon final states at the parton level and have been used to fix the fundamental scale parameter Λ of QCD.

However, already within perturbation theory it becomes clear that the binding forces are of long range and can not be accessed perturbatively. In the non-relativistic limit, perturbative 1-gluon exchange leads to a Coulomb potential. In such a potential the Bohr radius of $c\bar{c}$ is of order $\mathcal{O}(1$ fm) which clearly indicates the limits of a purely perturbative treatment.

The non-relativistic approach then provides a fairly direct way to cast one's knowledge, prejudices or ignorance about the strong binding forces at large distances into the form of a potential ansatz. After solving the corresponding Schrödinger equation, from a comparison of the calculated spectrum and other observables with the experimental findings one might then derive some picture of the confinement mechanism.

Indeed, this procedure has been a major source for information about the strong interactions at large distances during the last 20 years and certainly has lead to a more or less correct phenomenological description of heavy quark bound states. Nevertheless, it appears very desirable to also derive the basic properties of confining forces directly from the QCD Lagrangian without any further model assumptions. Such a quantitative non-perturbative analysis of QCD at large distances is, at least at present, provided only by the lattice approach.

In this little review I shall briefly recall some experimental and phenomenological knowledge about heavy quarkonia – more details about these aspects should be looked up and more complete lists of references can be found in review articles as e.g. Refs. 1.2.3 – and then concentrate on reviewing the results of lattice calculations concerning various aspects of interquark forces.

Certainly the most immediate problem is the existence and the form of the confining potential, section 2. Phenomenologically, this determines the gross features of the spectrum. There will be relativistic corrections to the central potential but, more important, an expansion in $1/m$ also introduces spin-dependent terms into the potential, dealt with in section 3. These terms lead to fine and hyperfine splittings in the spectrum which are sensitive to the Dirac structure of the confining forces. More insight into the confinement mechanism can be gained from a study of color field distributions between a static quark-antiquark pair, presented in section 4. Experimentally there is not much known in this area but detailed analyses of these distributions will possibly give evidence to whether the Nielsen-Olesen conjecture of confinement applies. Finally, section 5, at the current state of affairs almost meant as an outlook, will feature two investigations of forces between non-fundamental representations. This is an interesting subject insofar QCD should also be capable to describe nuclear forces and hadronic subsystems will eventually arrange themselves into non-fundamental representations of the color group.

Many lattice investigations so far have been carried out in the valence quark or quenched approximation which neglects virtual light quark loops. Phenomena which depend crucially on the dynamics of light quarks like e.g. eventually the breaking of a flux tube are thus not accessible by these studies. Basic properties of QCD which are dominated by the non-abelian gluon interaction, however, should and do survive the approximation. Thus, the quenched approximation serves as an important guide for many aspects of non-perturbative QCD. Of course, the

results of a pure glue theory must be checked by investigations in full QCD. It is thus reassuring to see reliable results beginning to emerge from simulations which include light dynamical quarks on reasonably large lattices, as will be seen in the following sections. Secondly, lattice studies frequently use $SU(2)$ instead of $SU(3)$ as the color gauge group because the numerical evaluation of the Feynman path integral is easier with less degrees of freedom. However, it is expected that the main features of non-abelian dynamics carry over from $SU(3)$ to $SU(2)$ and, indeed, in many cases even quantitative agreement between the two gauge groups has been found. Therefore, I shall also report on results obtained in the computationally simpler $SU(2)$ gauge theory.

2. Confinement Potential

At about the time of the J/ψ discovery [4] Appelquist and Politzer speculated that heavy quarks should form positronium-like bound states [5]. Led by asymptotic freedom they suggested to calculate the spectrum of these states from a Coulomb potential ansatz. It was however also clear from the beginning that long-range forces are utterly important. In the following quite a few ansätze for the potential were developed and discussed, with their predictions for spectrum and decay widths being compared to the increasing amount of experimental data.

The prototype ansatz is represented by the Cornell potential [6], which consists of a Coulomb-like part as in positronium, motivated by 1-gluon exchange at small distances, plus a long-range confining part which was taken to be linear in the quark-antiquark separation,

$$V(R) = -\frac{e}{R} + \sigma R \tag{1}$$

(Here, as in the following, R denotes the distance between the heavy quark-antiquark pair.) In the Cornell ansatz the "Coulomb" coefficient e is fixed to $\simeq 0.48$ and σ denotes the string tension, obtained from Regge trajectories and cooroborated by successful spectrum fits as $\sqrt{\sigma} \simeq 440$ MeV.

An elegant interpolation between a long-range linear term at one end and a Coulomb $1/R$ part with a perturbatively (to one loop order) running coefficient dominating at short distances is assumed in the Richardson potential [7].

$$V(R) = -\frac{4}{3}\frac{16\pi^2}{33-2N_F}\int\frac{d^3\vec{q}}{(2\pi)^3}e^{i\vec{q}\vec{x}}\frac{1}{\vec{q}^2\ln(1+\vec{q}^2/\Lambda^2)} \tag{2}$$

with the desired behavior at small and large distances,

$$\begin{aligned} R \text{ small}: V(R) &\rightarrow -\frac{4}{3}\frac{\alpha_s(R)}{R} \\ R \text{ large}: V(R) &- \Lambda^2 R \end{aligned} \tag{3}$$

The nice feature of the Richardson potential is this combination of perturbative and non-perturbative aspects with a dependence on just one free parameter Λ which is not directly related to the perturbative scale parameter but fixed empirically to $\Lambda = 398$ MeV $\simeq \sqrt{\sigma}$.

The so-called QCD potentials differ from the Richardson ansatz insofar that they incorporate perturbation theory to second order [8], at small R.

$$\begin{aligned} V(R) &= -\frac{4}{3}\frac{\alpha_s(R)}{R} \\ \alpha_s(R) &= \frac{4\pi}{b_0\ln(1/R^2\Lambda^2_{\overline{MS}})}\times\left[1-\frac{b_1}{b_0^2}\frac{\ln\ln(1/R^2\Lambda^2_{\overline{MS}})}{\ln(1/R^2\Lambda^2_{\overline{MS}})}+\frac{C}{\ln(1/R^2\Lambda^2_{\overline{MS}})}\right] \end{aligned} \tag{4}$$

with $b_0 = \frac{1}{3}(11N - 2N_F)$, $b_1 = \frac{1}{3}[34N^2 - N_F(13N^2-3)/N]$ and $C = (31N - 10N_F)/9b_0 + 2\gamma_E$ for $SU(N)$ and N_F flavors. At large R they typically assume a linear or square root dependence on the distance accompanied by varying interpolation prescriptions for intermediate quark-antiquark separations (for a list of references see e.g. Ref. 2).

Finally there are purely phenomenological potentials. A logarithmic ansatz [9]

$$V(R) = c_0 + c_1\ln(R/R_0) \tag{5}$$

is motivated by the observation that the $1S-2S$ mass differences in the $c\bar{c}$ and $b\bar{b}$ quarkonia are nearly independent of the quark mass. A simple power ansatz has been written down by Martin [10],

$$V(R) = a + b\,R^{0.1} \tag{6}$$

These expressions are not motivated by QCD but may serve as a means to test the sensitivity of the heavy quark spectrum on QCD ingredients.

The common feature of all these ansätze is the assumption of flavor independence of the quark potential. Indeed, this idea is supported in a model independent way by applying the inverse scattering method to extract a potential from the measured spectra [11].

The existence of a local potential has been questioned from within the sum rule approach. Energy level shifts due to the gluon condensate, $\Delta E_n \sim \langle G^2_{\mu\nu}\rangle n^3/m^3$, cannot be deduced from a local potential [12]. However, these shifts can reliably be calculated only at $Q\bar{Q}$ separations which are very small in comparison to the characteristic scale of the condensate [13]. There they are hard to identify because of their small size due to the dependence on the heavy quark mass m. Phenomenologically, this question can be analyzed by studying the mass (in)dependence of the potential down to the toponium range whereas theoretically the situation remains rather intricate at the moment. A possible clarification may come from lattice computations of a very heavy quarkonium spectrum both from a $Q\bar{Q}$ potential and from a direct mass evaluation. This would however require lattice spacings smaller than presently available.

A few representative examples of phenomenologically successful potentials are drawn in Fig. 1. In the figure also the r.m.s. radii of the lowest vector meson quarkonia are indicated. It is quite obvious that in the distance range 0.1 fm $\leq R \leq$ 1 fm, relevant for charmonium and bottonium physics, all potentials are in numerical agreement and show a basically logarithmic shape. Differences primarily lie in the

short distance behavior, which in future may be thoroughly tested by top quark bound states if the top quark is not too heavy [2]. However, for the present time, some information about the short distance properties of the potential is provided by quantities which depend on the wave function at the origin like e.g. the leptonic widths, $\Gamma_{ee} \sim |\psi(0)|^2$ and are sensitive to the shape at small R. Potentials with a logarithmically softened Coulomb singularity generally lead to smaller widths. Indeed the leptonic width calculated from the Cornell potential is off by a factor 2 whereas QCD like potentials are favored by the experimental data [4].

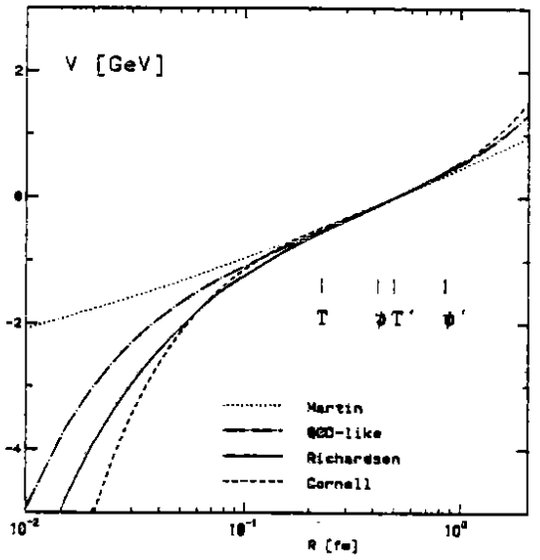

Figure 1: A representative sample of phenomenological potentials. As an example for a QCD like potential the ansatz of Ref. 14 was taken.

An important tool for the gauge-invariant definition of the interquark potential has been introduced by Wilson [15] (and in a different context by Wegner [16]). Therefore I shall briefly repeat the basic ideas. Consider a color singlet bound state M of a quark at x_1 and an antiquark at x_2,

$$\begin{aligned} M &= \bar{\psi}(x_1)\, P \exp\left(i \int_{x_1}^{x_2} dx_\mu G_\mu\right) \psi(x_2) \\ &= \bar{\psi}(x_1)\, U(x_1;x_2)\, \psi(x_2) \end{aligned} \tag{7}$$

which is gauge-invariant because of the insertion of path-ordered exponentials of gauge fields G_μ. In Euclidean metric, the time evolution of this state from $t = 0$ to $t = T$ is given, in path integral representation, by

$$\begin{aligned} \langle M(T) M(0)\rangle = & \int \mathcal{D}\psi \mathcal{D}\bar{\psi} DG_\mu \exp\left(-\int d^4x\, \mathcal{L}\right) \\ & \times\ S(\bar{x}_2, 0; \bar{y}_2, T) U(\bar{y}_2, T; \bar{y}_1, T) S(\bar{y}_1, T; \bar{x}_1, 0) U(\bar{x}_1, 0; \bar{x}_2, 0) \end{aligned} \tag{8}$$

where $S(x_1;x_2)$ denotes the quark propagator and $\mathcal{L}$ is the Lagrangian. In the static quark limit, the Dirac equation for the (static) quark propagator S_0,

$$\left[\gamma_0 D_0(x;[G]) + m\right] S_0(x;y) = \delta_4(x-y) \tag{9}$$

can be solved in closed form, leading, for $x_0 > y_0$, to

$$S_0(x;y) = e^{-m|x_0 - y_0|}\ U(x;y)\ \delta_3(\bar{x} - \bar{y})\ \frac{1+\gamma_0}{2} \tag{10}$$

Collecting all parts, the four-point function Eq. 8 becomes, in the static quark limit,

$$\langle M(T) M(0)\rangle \ \sim\ e^{-2mT}\ W(C) \tag{11}$$

where $W(C)$ is the famous Wegner-Wilson loop around a closed path C,

$$W(C) = \int \mathcal{D}G_\mu P \exp\left(i \oint_C dx_\mu G_\mu\right) \exp\left(-\int d^4x\, \mathcal{L}_G\right) \tag{12}$$

Here $\mathcal{L}_G$ denotes the pure Yang-Mills part of the Lagrangian*. On the other hand, by inserting a complete set of energy eigenstates into Eq. 8,

$$\begin{aligned} \langle M(T) M(0)\rangle &= \sum_n \langle 0|M(0)|n\rangle e^{-E_n T} \langle n|M(0)|0\rangle \\ E_n &= 2m + V_n(R) \end{aligned} \tag{13}$$

one arrives at an expression from which, by comparison with Eq. 12, the relation between the Wilson loop (for e.g. a rectangular path $C = R \times T$) and the ground state potential $V_0(R)$

$$W(R,T) \underset{T\,\text{large}}{\longrightarrow} \exp\left[-V_0(R) T\right] \tag{14}$$

can immediately be read off.

The Wilson loop approach is now easily adapted to lattice investigations. After Wick-rotating to Euclidean metric and discretizing space-time, path integrals as e.g. Eq. 12 become ordinary yet high dimensional integrals which are evaluated by means of Monte Carlo importance sampling methods. For an introduction into the technicalities of numerical lattice investigations see e.g. Ref. 17. Here I just wish to add two remarks:

* In full QCD i.e. if in addition to the heavy quarks also light quarks are taken into account the sketched derivation goes through unchanged. Only the heavy quarks are integrated out while the contribution of the light quarks to the path integrals Eq. 8 and Eq. 12 are kept.

The inclusion of dynamical quarks in a numerical lattice calculation is quite computer time consuming. Quarks are fermions and obey anti-commutation relations which are comprehensible to a computer only through matrix representations. Since coding each quark field as matrix is prohibitively memory consuming, one exploits the Gaussian nature of the quark contribution to the path integral and does the integration over quark fields analytically. This then gives the fermion determinant, as indicated in Eq. 15 for the case of the partition function,

$$\begin{aligned} Z &= \int \mathcal{D}\psi\mathcal{D}\bar{\psi}\mathcal{D}G_\mu \exp\left\{-\bar{\psi}(D+m)\psi\right\} e^{-F^2_{\mu\nu}} \\ &= \int \mathcal{D}G_\mu \det\left\{D+m\right\} e^{-F^2_{\mu\nu}} \end{aligned} \tag{15}$$

The determinant cannot be calculated directly because of numerical stability problems. However, there are ways to incorporate it in a numerical simulation exactly. Still, this requires a computational effort which is larger by two or three orders of magnitude. Therefore, many calculations make use of the quenched approximation which consists of setting the determinant equal to the identity. This amounts to neglecting virtual (light) quark loops and thus the response of gluons to the quark dynamics. Judging from the success of the quark model one might expect this approximation to be qualitatively and, within 20 %, even quantitatively correct for observables which are dominated by gluon dynamics. Of course, this has to be checked by simulations of full QCD and it is therefore appealing that the present status of lattice technology allows us to start investigating the effect of light quarks on a more than exploratory level. Naturally the quenched approximation has to fail when quark dynamics is important. Even so, it serves as an important guide in the understanding of long range QCD forces.

In the second remark I want to recall that all lattice calculations are performed at finite lattice spacing a. This introduces a certain coarseness in the (spatial) resolution and, moreover, breaks continuous continuum symmetries down to discrete lattice ones. Rotational invariance under only discrete angles is one of the most obvious examples. Long-distance physics however will only very weakly be sensitive to the distortions caused by the the lattice coarseness at small scales. It is therefore mandatory that the lattice spacing is much smaller than the typical size of the system under consideration, e.g. $a << 1/m$, the Compton wave length of a hadron with mass m. In this case of long-distance quantities it is then possible to extract continuum properties of the theory, in particular if asymptotic scaling behavior is verified in observables with non-trivial (mass) dimension, like e.g. the string tension,

$$(\sqrt{\sigma}a)_{lat} = (\sqrt{\sigma})_{phys} \times \frac{1}{\Lambda_L}\left(\frac{16\pi^2}{b_0 g_0^2}\right)^{\frac{b_1}{2b_0^2}} \exp\left\{-\frac{3\pi^2}{b_0 g_0^2}\right\} \tag{16}$$

Here, as in Eq. 4, b_0 and b_1 are the first two coefficients in the perturbative β function for $SU(N)$ and N_F flavors, g_0 is the bare coupling constant and Λ_L denotes the fundamental scale parameter of QCD in the lattice regularization. Thus the renormalization group tells us how the continuum limit is reached and it is not necessary to really run at vanishing a as long as the lattice spacing is small enough. Even though there are $O(a)$ corrections to Eq. 16, which at current values for the coupling constant are not negligible*, these corrections appear to be universal and therefore cancel in ratios like e.g. $a\sqrt{\sigma}/am_{nucleon}$. Reliable continuum numbers for long-range properties can therefore be extracted from those ratios. On the other hand, it is rather difficult to investigate in short distance physics on the lattice. For the condition "a much smaller than the typical size of the physical system" to hold for distances less than say 0.1 fm one would have to go to very small lattice spacings. Yet also the size of the whole lattice needs to be bigger than e.g. a typical hadron in order to fix the scale via a non-perturbative quantity†. With the currently available computer resources one may be just on the verge to achieve short and long physical distances with enough resolution at the same time. Still, at small R one should be prepared for distortions due to lattice coarseness artefacts and to lattice symmetries being not yet restored to the continuum ones.

Coming now to the lattice results on the confinement potential, it is impossible to discuss all the contributions to this field [21–32]. The confinement hypothesis has been the subject of the earliest attempts in numerical lattice investigations starting in 1979 with the famous attempt of Creutz [21] in quenched $SU(N)$ on lattices of size 5^4 (!). Today's lattices are as large as 36^4 in quenched $SU(3)$ [29] and $48^2\times 56$ in quenched $SU(2)$ [30]. Much effort has gone not only into increasing the lattice size but also into developing improved techniques to extract the ground state potential. The main progress has been the construction of operators M which have a large overlap with the ground state so that the limit $T \to \infty$ as in Eq. 14 is no longer required because the correlation function is dominated by V_0 already at smaller T values [33].

The result of a recent quenched $SU(3)$ investigation [28] which is able to reach distances almost up to 2 fm is shown in Fig. 2. The plot combines data obtained at three different values of the coupling constant which have been successfully mapped onto each other via the (non-asymptotic) scaling of the string tension. In addition to planar Wilson loops, it is customary to analyze also loops where quark and antiquark are not connected by a straight path on the lattice but lie on opposite edges of rectangles as well as cubicles. This way the restoration of rotational symmetry can be tested. It turns out that at large distances rotational invariance holds quite well while at smaller separations a correction of known lattice artefacts, i.e. a replacement of the continuum Coulomb term $1/R$ by the lattice gluon propagator [22],

$$\frac{1}{R} \to \sum_{\vec{p}\neq 0} \frac{\cos(\vec{p}\vec{R})}{4\sum_i \sin^2(p_i/2)} \tag{17}$$

is important. The data as shown in Fig. 2 exhibit a linear increase at large distances

* For some results of a program initiated by Symanzik [18] to eliminate these corrections in first order see e.g. the talk by Kenway, these proceedings [19].

† A method to combine short and long distance QCD on the lattice in a stepwise manner has been suggested in Ref. 30.

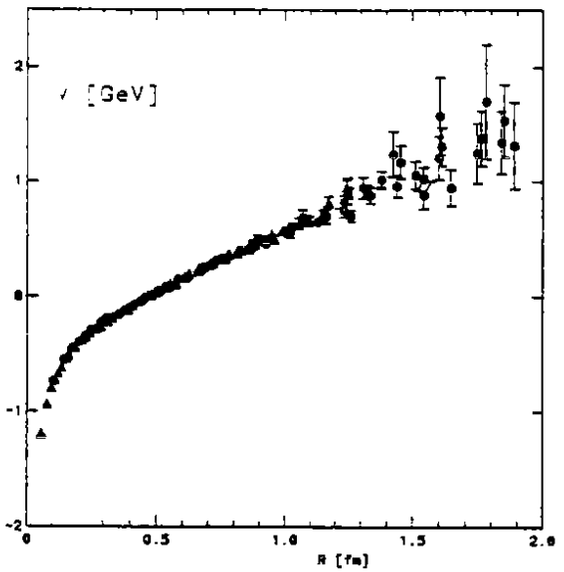

Figure 2: The potential in quenched $SU(3)$ (data obtained from Ref. 28).

beyond any doubt. This result as well as observations in earlier attempts represent important support for the confinement hypothesis.

The linear rise at large distances is accompanied by a Coulomb-type behavior at small R. It is now very tempting to analyze the short distance behavior in more detail, keeping in mind the above mentioned caveats. At not too small quark-antiquark separations, for most lattice data* the coefficient e of the Coulomb term is compatible with the prediction of bosonic string models of a universal strength [36] $e = \pi/12$ (see also section 4.). Being a typical non-perturbative effect this might not be too surprising at large distances. However, at small separations one would like to make contact with perturbation theory by seeing $e = \frac{4}{3}\alpha(R)$ and $e = \frac{3}{4}\alpha(R)$ for $SU(3)$ and $SU(2)$ resp. following the perturbative prediction [5]. This would allow one to fix the renormalized coupling constant directly from a physical quantity and to determine the scale parameter Λ from its dependence on R. This is a better choice [37] than taking Λ from a long-range quantity as e.g. $\sqrt{\sigma}a$ via Eq. 16 because, in the bare coupling, scaling but not yet asymptotic scaling is observed at current values of g_0. In order to inspect the short distance behavior of the potential more closely it is useful to compare the data with the string model prediction $-\pi/12R+\sigma R$ where the string tension has been obtained from fits with this expression at large R. Fig. 3 shows quite clearly that at small values of R, below 0.2 fm, deviations from this behavior are beginning to emerge. Inspecting these deviations quantitatively there are indications that indeed the Coulomb coefficient starts "running" according to perturbation theory [38]. If the extracted behavior of $\alpha(R)$ is turned into a value of the scale parameter the data lead to results for $\Lambda_{\overline{MS}}^{N_f=0}$ between 200 and 300 MeV, for $SU(2)$ [28,30] as well as $SU(3)$ [28,29]. It is presumably premature to quote a more precise (statistical) error because the main uncertainty are possible systematic effects coming from unknown lattice artefacts beyond the corrections according to Eq. 17. It should, however, be mentioned that other (quenched) approaches [39] are also pointing to the same interval.

* Potentials obtained from correlations of Wilson-Polyakov lines i.e. flux lines wrapping around the periodic lattice lead to somewhat different values for the Coulomb coefficient [27] (and also for the string tension). This might be due to unresolved admixtures of excited string states [34], see also Ref. 35.

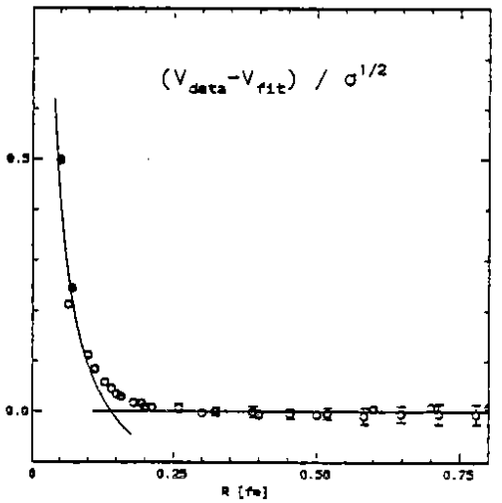

Figure 3: Deviations of the quenched $SU(2)$ potential at short distances from the string model behavior $V_{fit} = -\pi/12R + \sigma R$ which describes the data at large R. The curve at small separations is the perturbative prediction for $\Lambda_{\overline{MS}}^{(0)} = 200$MeV. The data is taken from Refs. 38 and 30.

At this point it must be emphasized that the presented numbers stem from simulations of the pure glue theory. The value for $\Lambda_{\overline{MS}}$ will change when quarks are present. One should also recall that the scale had been set by equating the lattice string tension to the experimental value, i.e. to its value in a world with quarks. This might be the reason for the 20% discrepancy between the lattice data

and phenomenologically successful potentials. It must therefore be appreciated that results from investigations in the full theory are coming in.

The main qualitative change, which is hoped to be borne out from studies with dynamical quarks, is a breaking of the flux tube. For large distances > 1 fm, the color charges of the heavy quarks are expected to be screened by the spontaneous creation of light quark-antiquark pairs. As a result, heavy-light mesons can be formed, and the interquark potential should flatten out at distances near a typical hadron size and finally turn over to a Yukawa-type potential between the mesons. At present however, the lattice sizes in full QCD are not yet as large as in quenched analyses. The most advanced effort so far in this direction [32] is reaching distances up to $R \simeq 1.0$ fm and does not see indications of a flattening off, Fig. 4. This is also not expected to happen in the investigated distance range. On the contrary, the full QCD data confirms a Coulombic plus linear rise between 0.1 and < 1 fm quite nicely and thus supports standard heavy quarkonium spectroscopy. Again, in Fig. 4 two different data sets at different values for the bare coupling constant have been mapped onto each other confirming scaling in the string tension. Also it was checked that rotational invariance has been restored.

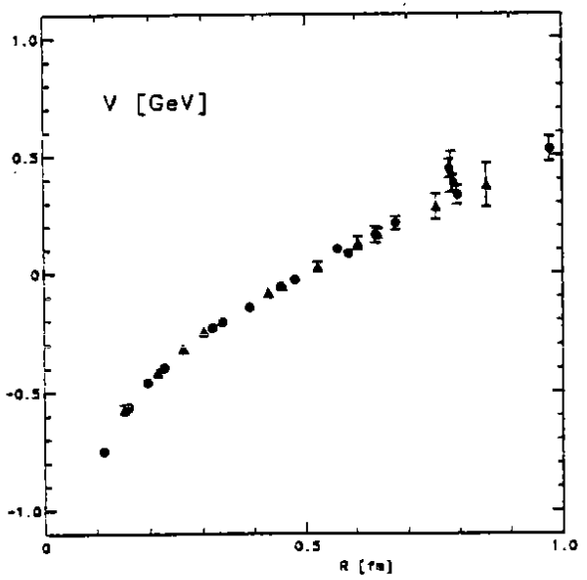

Figure 4: The potential in full $SU(3)$. The results were obtained with quark masses of $\simeq$ 35 MeV. Circles and triangles denote data from different values of g_0. (Data taken from Ref. 32.)

In summary, quenched as well as full QCD lattice analyses show a Coulomb plus linear behavior of the interquark potential at quark-antiquark separations $0.1 \leq R \leq 1.0$ fm in accordance with heavy quarkonium phenomenology. Smaller lattice spacings are desireable to determine the running strong coupling constant more precisely. At the other end, larger lattice sizes are necessary to establish flux breaking due to spontaneous creation of light quark pairs.

3. Spin-dependent Potential

Spin-dependent terms of the potential lead to fine and hyperfine splittings in quarkonium spectra. Beyond their phenomenological importance they are of particular interest because their dependence on the spin structure of the Bethe-Salpeter kernel allows one to gain some deeper understanding of the nature of the confining forces.

The general form of the spin-dependent terms is derived from a systematic expansion in $1/m$ of the corrections to the non-relativistic Schrödinger equation. The result up to $\mathcal{O}(1/m^2)$ is the generalized Breit-Fermi Hamiltonian with

$$\begin{aligned} V_{spin}(R) = & \frac{1}{2m^2 R} \; \vec{L}\vec{S} \; (V_0' + 2V_1' + 2V_2') \\ & + \frac{1}{m^2} \; [\frac{1}{R^2} (\vec{R}\vec{S}_1)(\vec{R}\vec{S}_2) - \frac{1}{3}\vec{S}_1\vec{S}_2] \; V_3 \\ & + \frac{2}{3m^2} \; \vec{S}_1\vec{S}_2 \; V_4 \end{aligned} \tag{18}$$

here written for the case of two identical quark masses m. $\vec{S}_{1,2}$ are the spin vectors of quark 1 and 2 resp., $\vec{S} = \vec{S}_1 + \vec{S}_2$, $\vec{L}$ is the total angular momentum and V_0 the ground state potential. The new potentials V_i, $i = 1, \ldots, 4$ can not be calculated within the Bethe-Salpeter approach. However, a spin decomposition of the kernel into invariants

$$S\, 1 \otimes 1 + P\, \gamma^5 \otimes \gamma_5 + V\, \gamma^\mu \otimes \gamma_\mu + A\, \gamma^\mu\gamma^5 \otimes \gamma_\mu\gamma_5 + T\, \sigma^{\mu\nu} \otimes \sigma_{\mu\nu} \tag{19}$$

reveals that the various confining parts S, P, V, A and T contribute quite differently to the spin-dependent potentials. For scalar and vector confinement the contributions are given in the following table.

	V_0	V_1	V_2	V_3	V_4
scalar	S	$-S$	0	0	0
vector	V	0	V	$\frac{1}{R}V' - V''$	ΔV

As a result, the scalar spin-orbit term $V_{LS}^{(S)} \sim -V_0$ differs clearly from the one obtained if vector confinement holds, $V_{LS}^{(V)} \sim +3V_0$. For a pseudoscalar kernel there is no static potential at all, while axialvector and tensor both lead to a spin-dependent static potential. Those options are clearly not in accordance with the experimental findings.

The spin-dependent potentials can be related to expectation values of chromo-electric and chromo-magnetic fields within the Wilson-loop approach [10]. An expansion in $\vec{r}\vec{D}$, the spatial part of the covariant derivative, of the full quark propagator around the static limit, Eq. 9, reproduces the Breit-Fermi Hamiltonian Eq. 18, with the coefficients V_i given by insertions of color fields into the Wilson loop at the positions of quark and antiquark*

$$\begin{aligned}
\frac{R_k}{R}V_1'(R) &= \frac{g^2\epsilon_{ijk}}{2T}\int\int(t'-t)\langle B_i(\vec{0},t)E_j(\vec{0},t')\rangle_W\,dtdt'/\langle 1\rangle_W \\
\frac{R_k}{R}V_2'(R) &= \frac{g^2\epsilon_{ijk}}{2T}\int\int(t'-t)\langle B_i(\vec{R},t)E_j(\vec{0},t')\rangle_W\,dtdt'/\langle 1\rangle_W \qquad (20)\\
\left(\frac{R_iR_j}{R^2}-\frac{\delta_{ij}}{3}\right)V_3(R)+\frac{\delta_{ij}}{3}V_4(R) &= \frac{g^2}{T}\int\int\langle B_i(\vec{0},t)B_j(\vec{R},t')\rangle_W\,dtdt'/\langle 1\rangle_W
\end{aligned}$$

The brackets $\langle..\rangle_W$ denote expectation values of operators attached to the Wilson loop, for example $\langle 1\rangle_W$ is the Wilson loop itself.

Based on the assumption of electric confinement it has been argued that magnetic fields are only perturbatively correlated and that correspondingly all spin-dependent potentials are short-ranged. However, Gromes could proof that Lorentz invariance implies a relation between the ground state potential and the first two spin terms,

$$V_2 - V_1 = V_0 \qquad (21)$$

with the consequence that not both, V_1 and V_2 can be short-ranged [41]. The proof is based on the transformation properties of magnetic and electric fields, e.g. $\vec{E}' = \vec{E} = \vec{v}\times\vec{B}$ under a boost. Thus, in the expression Eq. 20 for V_2, one can switch to a frame where the quark at position $\vec{0}$ is moving now thereby removing the electric field. The same possibility does not exist for V_1 where both E and B field are sitting on the same quark. In this modified version the argument about short-ranged purely magnetic correlations may hold and suggest that V_1 contains a long-range part.

Experimentally, the situation is such that the fine and also the hyperfine splittings in the b sector allow one to distinguish between vector and scalar confinement. A quantity which is particularly sensitive to the Lorentz structure of the potential is the ratio R_{FS} of ${}^3P_J$ fine splittings,

$$R_{FS} = \frac{M({}^3P_2)-M({}^3P_1)}{M({}^3P_1)-M({}^3P_0)} \qquad (22)$$

In Table 1 the experimental results are compared with theoretical predictions based on a scalar linear confining part plus a perturbative vector part including next-to-leading QCD corrections [42]. Vector confinement which leads to values of $R_{FS} > 0.8$ appears to be ruled out. Scalar confinement is favored although a short-range spin-orbit term coming about by a cancellation of long-range contributions to both V_1 and V_2 is not yet excluded by the data [1].

* There are alternative methods for which we refer to the review Ref. 3.

Table 1: Fine splittings. ΔM_{FS} is defined as $\Delta M_{FS} = M({}^3P_2) - M({}^3P_0)$. The table is reproduced from Ref. 1.

P States	χ_c	$\chi_b(1P)$	$\chi_b(2P)$
Scalar Confinement			
R_{FS}	0.46	0.68	0.70
ΔM_{FS}[MeV]	145	42	34
Experiment			
R_{FS}	0.48 ± 0.01	0.67 ± 0.06	0.58 ± 0.06
ΔM_{FS}[MeV]	145 ± 1	53 ± 2	39 ± 2

At this point it should perhaps be noted that higher-order perturbative QCD corrections [43] also lead to a logarithmic mass dependence of the potentials and, for unequal quark masses, to an additional term V_5. Both aspects are not foreseen in the approach of Ref. 40 which does not contain any approximation as far as α_s corrections are concerned. Presumably the problem arises because Ref. 40 considers quark propagators in a fixed background gluon field and possible renormalization effects need to be clarified further.

The potentials V_i can be calculated on the lattice. To this purpose the expressions Eq. 20 are carried over. The color field insertions are approximated by plaquette terms e.g. for the plaquette in the x-y plane

$$U_{xy} = 1 + iga^2\mathcal{B}_z + \mathcal{O}(a^3) \;\Rightarrow\; gB_z \simeq \frac{1}{2ia^2}\left(U_{xy} - U_{xy}^\dagger\right) \qquad (23)$$

giving rise to the "ears" of the Wilson loop. There are some subtleties concerning the subtraction of the self-energies of the quarks which are associated with the perimeter $L(C)$ of the loop. For smooth, non-intersecting loops it could be proven [44] that these contributions factorize,

$$W(C) \sim \exp\left(-cL(C)/a\right) W_{ren}(C) \qquad (24)$$

leaving a well-defined renormalized Wilson loop W_{ren} in the continuum limit. If field operators are inserted it has been shown to $\mathcal{O}(g^2)$ in pure gauge theory [45] that the self-energies can be removed according to, in short-hand notation,

$$\langle B_zB_z\rangle_W^{ren} = \frac{\langle B_zB_z\rangle_W\langle 1\rangle_W}{\langle U_{xy}\rangle_W^2} \qquad (25)$$

and similarly for the other components. In these ratios factorizing self-energy terms would also cancel in higher orders.

There have been a few lattice investigations of the spin-dependent potentials both in color $SU(2)$ and $SU(3)$ (and a feasibility study in $U(1)$ [46]). Most of them were carried out in the quenched approximation [45,47,48] with only two studies recently in

full QCD [49,50]. After an initial irritation, since the work of Ref. 47 all quenched lattice results favour a long-range part residing in V_1. This also holds true for the most advanced attempt in full QCD [50], the results of which are shown in Fig. 5. Here additionally the restoration of rotational symmetry was investigated. The figure shows quite clearly that the derivative of the spin-orbit potential, dV_1/dr is flat within the error bars, strongly favouring the long-range confining part residing in V_1. The other spin-orbit potential, dV_2/dr, as well as the tensor force V_3 drop rapidly. In fact, they appear to be well described by one-gluon exchange, demonstrated by the dotted lines. Of course, within the precision of the data a small long-range part in V_2 cannot entirely be excluded. The spin-spin term V_4 is practically zero for distances larger than $\sqrt{2}a$ which is compatible with the (smeared) perturbative behavior $V_4(R) \sim \delta(R)$. Compared with the static potential V_0, the data meets the Gromes relation only up to within 30 %, which is presumably due to higher order self-energy terms not completely cancelled in the normalization. Still, it can be safely concluded that the lattice results very strongly support the confining potential to be predominantly of scalar origin.

4. Profiles of the Flux Tube

The physical picture of confinement has strongly been influenced by a supposed analogy to the Nielsen-Olesen string [51]. The QCD vacuum is thought to be similar to a superconductor of the second kind. Like a superconductor tries to expel magnetic flux due to the Meißner effect, it is expected that chromo-electric flux lines, which originate from color charges brought into the vacuum, are squeezed into a flux tube. At large distances, this would cause a constant energy density per unit length of the flux tube and thus a potential which rises linearly with the separation between two color charges. Corresponding to normal conductivity inside cavities of magnetic flux inside a superconductor, the interior of a color electric flux tube is thought to be built-up on a perturbative vacuum i.e. to be asymptotically free. These conjectures have lead to the construction of various models, above all bag and string models. It is now interesting to compare these models to results which come from a non-perturbative treatment of QCD.

As mentioned, string models first of all feature a linear rise of the interquark potential at large $Q\overline{Q}$ separations. Moreover, oscillations of the string in the direction perpendicular to the line connecting the two quarks induce a $1/R$ term with a strength $(d-2)\pi/24$ (in d dimensions), which is independent of the underlying gauge group [36]. Thus in 4 dimensions one has a potential

$$V_{string} = -\frac{\pi}{12}\frac{1}{R} + \sigma R \tag{26}$$

Quite clearly, this Coulomb-like term is a long-range phenomenon and is expected to describe the data only at large quark separations. The range of applicability has been made more quantitative [52] with the result that the string picture should be valid for distances larger than $R^2 \geq \pi(d-2)/12\sigma$ which amounts to roughly $R \geq 0.3$ fm.

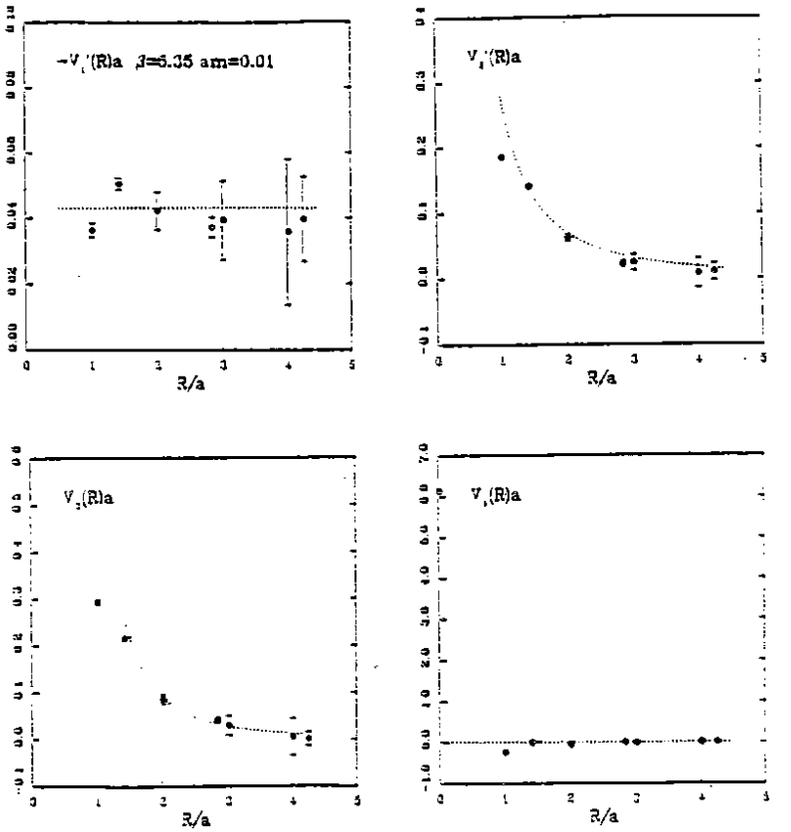

Figure 5: The spin-dependent potentials in full QCD. The results were obtained with a quark mass of $\simeq 35$ MeV, the lattice spacing is $\simeq 0.12$ fm (taken from Ref. 50).

From bag models on the other hand it is known that a linear rise may set in already at rather small quark separations [53].

Within the lattice approach we have seen before that at small to intermediate distances the data is quite well described by the universal string correction. In addition, a detailed comparison with string models has been the target of a series of lattice studies a few years ago [54]. In these papers different gauge groups were analyzed, with particular emphasis on studies in only $2+1$ dimensions. There the perturbative Coulomb term has a logarithmic $\ln R$ behavior instead of the more

familiar $1/R$ in $3+1$ dimensions, which makes the isolation of the string term somewhat more easy. The main result is a confirmation of the universal strength of the Coulomb-like term and, more generally, of the string model at distances which are larger than the lower bound given above.

A more detailed picture of the structure of the flux tube is provided by analyses of field strength distributions between two heavy quarks [55–58,25]. To this end one usually takes the plaquette as a sensor for chromo-electric and chromo-magnetic fields [57],

$$\begin{aligned} E_i^2 &\sim \mathcal{R}\,\{tr(U_{i4}-1)\} \\ B_k^2 &\sim \epsilon_{ijk}\mathcal{R}\,\{tr(1-U_{ij})\} \end{aligned} \tag{27}$$

$(i,j,k = 1,2,3)$ and correlates these operators with the Wilson loop. By suitably choosing the orientation of the plaquettes one can disentangle the field strength components parallel and perpendicular to the line connecting the heavy quark-antiquark pair. Changing the position of the operator insertions relative to the loop then allows to obtain entire profiles of the spatial field distribution. The numerical determination thereof is hampered by considerable noise effects. Thus the best results obtained so far originate from quenched $SU(2)$ simulations, where elaborate noise reduction techniques could be applied [26,58]. Pure $SU(3)$ data [56,57] is scarce. Here new attempts which incorporate improved smearing methods would certainly improve this situation.

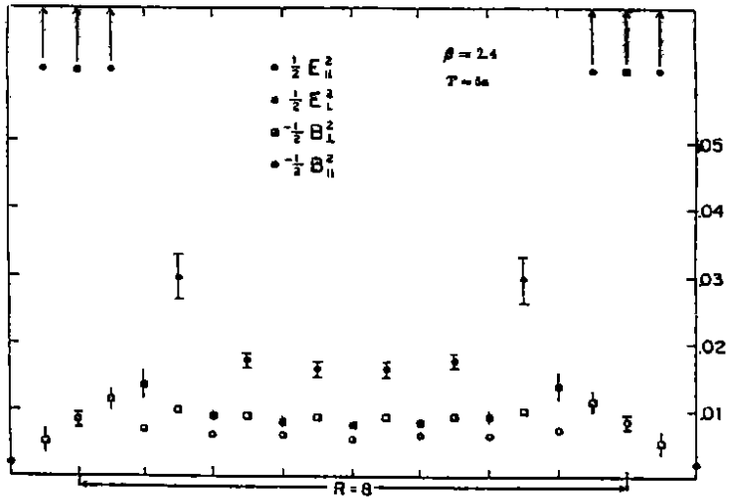

Figure 6: The longitudinal profile of the flux tube for all components. (Taken from Ref. 58.)

The numerical lattice results are as follows: The magnetic field strength components are consistently negative, relative to their vacuum values. This conforms with the expectation that magnetic flux is expelled from the flux tube. Ordered by absolute value, the parallel electric component is always largest, with the perpendicular electric and perpendicular magnetic components being next and comparable in absolute value. The parallel magnetic contribution is always smallest, yet even at fairly large quark-antiquark separations still different from zero, Fig. 6. The field strength distribution, as function of the perpendicular distance to the line connecting the quark pair, is shown in Fig. 7 and seems to follow rather an exponential decrease

$$\bar{E}^2, \bar{B}^2(x_\perp) \sim \exp(-x_\perp/\lambda) \tag{28}$$

than a Gaussian or Coulomb behavior. (Here and in the following it is understood that the field strength operators are inserted into Wilson loop expectation values, with vacuum contributions properly subtracted.) This is to be confronted with the string model result [59] which predicts a Gaussian decrease

$$\bar{E}^2(x_\perp) \sim \exp(-x_\perp^2/\langle x_\perp^2\rangle) \tag{29}$$

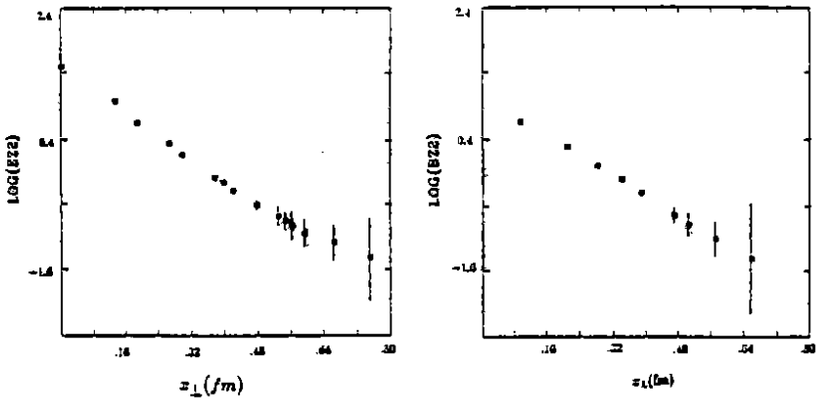

Figure 7: The transverse profile of the flux tube for $E_\parallel$ (a) and $B_\parallel$ (b) at the midpoint between the two heavy quarks. (Taken from Ref. 58.)

A very important quantity is the energy density inside the flux tube,

$$\epsilon(x) = \frac{1}{2}[\bar{E}^2(x) + \bar{B}^2(x)] \tag{30}$$

The magnetic contributions, being negative, cause large cancellations and make this not an easy quantity to measure. Still, the numerical value of about $\epsilon \simeq 4$ GeV/fm^3,

extracted from the lattice, turns out to be an order of magnitude larger than a typical density in the MIT bag model [53]. It is difficult to imagine any reason why the lattice number should be off by such a large factor. Furthermore, the determination of the energy density can be checked for intrinsic errors by a comparison with the confinement potential via the energy sum rule [60]

$$\frac{1}{2}\sum_{\vec{x}}(\vec{E}^2+\vec{B}^2)(\vec{x}) = V_0(R) + V_{self} \tag{31}$$

This sum rule can also be exploited in a differential fashion by restricting the sum over $\vec{x}$ to a spatial slice perpendicular to $\vec{R}$ and comparing the result with the increase in the potential when the quark separation is increased by one lattice unit. Then also the self-energy contribution V_{self} drops out. Both checks have, of course, been done and support the above given value for the energy density. The latter can then be used to define an average width of the flux tube by

$$\langle x_\perp^2\rangle_\epsilon = \frac{\int d^2x_\perp x_\perp^2 \epsilon(x_\perp)}{\int d^2x_\perp \epsilon(x_\perp)} \tag{32}$$

for which the data indicates a constant behavior as a function of R, with a quite small value

$$\langle x_\perp^2\rangle_\epsilon^{1/2} \sim const \sim 0.2 \text{ fm} \tag{33}$$

Again, this is supported by the sum rule being saturated at small values of $x_\perp$ already. Quite contrary, string models predict for the width of the (vibrating) string a dependence on the quark pair separation according to

$$\langle x_\perp^2\rangle = \frac{1}{\sigma\pi}\ln R \tag{34}$$

On the other hand, estimating the width of the action density $\omega = \frac{1}{2}(\vec{E}^2-\vec{B}^2)$ yields numbers which are in agreement with such a logarithmic dependence. A reason for this difference between action and energy is not known.

In summary, (quenched) lattice results support the Nielsen-Olesen conjecture of electric confinement and seem to favor a rather broad action distribution but a narrow cigar-shaped energy distribution.

Naturally, these results have to be confirmed by an analysis in full QCD. However, the energy contained in the flux tube can now be shared between gluon and fermion contributions, the latter having been consistently neglected in the (quenched) sum rule Eq. 31. Moreover, at large quark-antiquark separations the flux tube is expected to break due to the presence of light (dynamical) quarks. The potential energy of the string should be consumed to create quark pairs which then screen the heavy quark color charges, the basic mechanism in jet fragmentation. Presumably such a phenomenon is announced by an increased probability to find (light) quark pairs inside the flux tube. At the current stage it is not yet feasible to thoroughly study the flux breaking (see the remarks in section 2). Nevertheless, first analyses of gluon distributions inside the flux tube in the presence of light quarks are under way, while some results about fermionic distributions are available [61,62]. The formation of a (chiral) $\bar{q}q$ density is an interesting question in regard to the nature of the vacuum which is realized inside the flux tube. While there is ample evidence that chiral symmetry is spontaneously broken in QCD, signalled by a non-vanishing value of the quark condensate in the vacuum $\langle 0|\bar{q}q|0\rangle$ (see e.g. Ref. 63 for a recent full QCD investigation), the Nielsen-Olesen conjecture suggests that inside the flux tube a trivial vacuum is restored. That would be indicated by a vanishing value for the quark condensate. First work on this subject was published by the Wien group [61]. However, they worked at rather large physical temperatures. A recent study on large lattices obtains different results [62]. Fig. 8 shows quite nicely that quarks do feel the color flux over the whole length of the flux tube. The perpendicular distribution seems to be rather narrow. Inside the flux tube the chiral density $\bar{q}q$ is smaller than its value in the vacuum, a trend which lends some support to the idea of a perturbative vacuum being restored inside the tube.

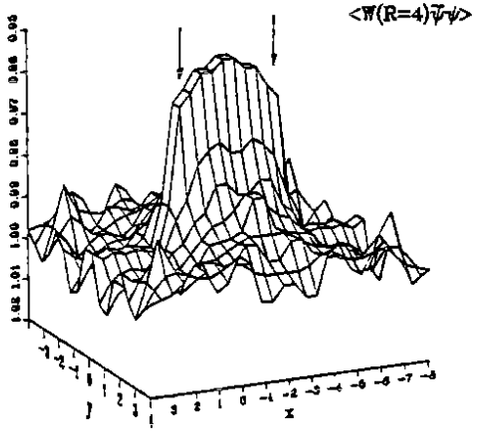

Figure 8: The fermionic profile $\langle\overline{Q}Q|\bar{\psi}\psi|\overline{Q}Q\rangle$ of the flux tube, normalized to the vacuum value $\langle\overline{Q}Q|\overline{Q}Q\rangle\langle 0|\bar{\psi}\psi|0\rangle$. The location of the heavy quarks is indicated by the arrows. Errors are of the size of the fluctuations outside the flux tube. (Taken from Ref. 62.)

5. Forces between non-fundamental Representations

QCD should not only describe the elementary interactions between quarks and gluons but also be capable of explaining the strong forces exchanged inside nuclei. There is a vast amount of literature about how to derive nuclear forces from QCD (for a discussion and references see e.g. Ref. 3). Here I can only concentrate on lattice attempts in this direction. There have been a few studies of forces between

non-fundamental representations, most of which however have to be regarded more or less as feasibility studies. In the following I shall elaborate on just two examples which apparently have reached a more advanced status.

The first example deals with the adjoint representation in the static approximation. This is studied by means of a modified Wilson loop, where the color flux lines have been arranged such as to describe a static color octet propagating only in time [54,24,25]. The potential between two such sources can then be obtained in the usual way. There are three main questions which can be answered from such an investigation. The first one is whether the potential is attractive at all. The second one addresses the problem whether the adjoint potential is just given by the fundamental one modified by the appropriate ratio of Casimir factors $2N^2/N^2-1$. Thirdly, the adjoint potential can be regarded as a model example of how screening can look like, of whether there is a gradual turn over into a short range Yukawa type potential or an abrupt change. The adjoint system is suitable for such a study already in the quenched approximation as a color octet unlike a quark can be screened by gluons alone. The most recent analysis [65] of these questions has been carried out in $SU(2)$ and the results are summarized in Fig. 9.

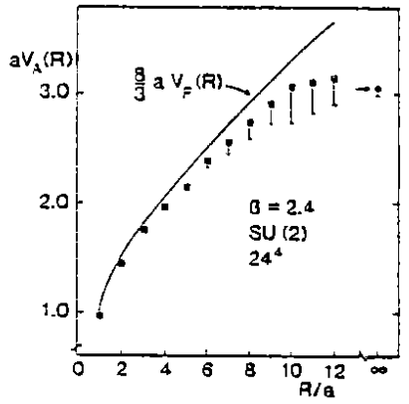

Figure 9: The adjoint potential between static sources. The data points are upper limits with statistical errors smaller than the size of the symbols. The lower error bars are estimates of the systematic error in the extrapolation to large T to obtain the ground state energy. The point at $R = \infty$ is twice the gluelump mass. Setting the scale with the string tension gives $a = 0.12$ fm. (Taken from Ref. 65.)

Quite clearly, there is an attractive potential between two color octets. Moreover, the data are precise enough to distinguish between a modified fundamental potential, $8/3V_F$ for $SU(2)$, and a genuine adjoint potential. As it turns out, the data favour a ratio of 2 rather than 8/3 between V_F and V_A. If this number carries over to $SU(3)$ that would lend some support to the Lund picture of gluon fragmentation. However, this would also be hard to really verify in an $SU(3)$ lattice analysis where the Casimir ratio is 9/4. Finally, in the accessible distance range up to $\simeq 1$ fm the potential data do not yet show a flattening off which would indicate screening to set in. The distance where this finally should happen can be estimated from the energy of two dissociated octets. This number is given by twice the mass of the lightest gluelump and is indicated in Fig. 9 by the rightmost data point. The two gluelump state becomes lighter than the energy stored in the adjoint string only at distances $R \geq 1$ fm, which is also roughly the size of a gluelump [66], so that screening effects are not yet visible.

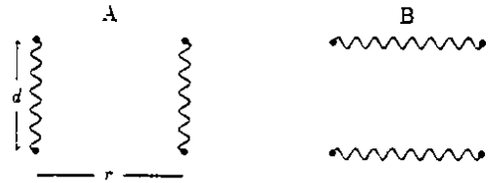

Figure 10: The two possibilities to combine four quarks into two separate mesons.

The second example are the forces exchanged in a four-quark system [67,68]. Again, the quarks are fixed in their spatial position. As indicated in Fig. 10 there are two ways to arrange flux lines such as to obtain two separate $Q\overline{Q}$ systems. The question to be asked is then whether the lowest energy state is just given by twice the fundamental potential V, implying that there is no interaction between the two quark-antiquark pairs. To the contrary, the second column of Table 2 indicates that the minimum energy is not much, but still significantly less than two times V. Such an interaction is often assumed to be derivable from two-body potentials including an exchange potential V_E, which is perturbatively motivated through color rearrangements. To calculate this interaction potential, V_4, one solves

$$\det\left\{\begin{pmatrix} 2V(d) & f\Delta V \\ f\Delta V & 2V(r) \end{pmatrix} - \lambda \begin{pmatrix} 1 & f/2 \\ f/2 & 1 \end{pmatrix}\right\} = 0 \qquad (35)$$

for $\lambda = V_4$ where $\Delta V = V(d) + V(r) - V_E$. Perturbatively, the overlap factor f, defined by $\langle A|B\rangle = \frac{1}{N}f$ is unity. However, if one uses the full two-body potentials including the long-range linear parts, the solution of Eq. 35 with $f = 1$ typically yields too large long-range Van der Waals-forces. Here, V_4 is known from the lattice data and one can solve for the overlap factor [68]. The resulting f-values are given in the third column of Table 2. They are certainly smaller than the perturbative number and decrease with growing distances r and d. Thus there is a genuine 4-body term exhibiting a rather short-ranged attractive force.

To summarize, the results on forces between non-fundamental representations indicate deviations from a behavior suggested by perturbative or color-

Table 2: The four quark binding energy in lattice units for quarks at the corners of a rectangle $r \times d$. f is the overlap factor described in the text. (Reproduced from Ref. 68.)

(d, r)	$V_4(d, r) - 2V(d)$	f
(1, 1)	−0.0695(5)	0.887(3)
(1, 2)	−0.0026(2)	0.868(3)
(2, 2)	−0.0582(2)	0.787(4)
(2, 3)	−0.0056(3)	0.709(15)
(3, 3)	−0.054(1)	0.666(4)
(3, 4)	−0.006(1)	0.53(3)
(4, 4)	−0.050(1)	0.502(4)
(5, 5)	−0.047(1)	0.34(1)
(6, 6)	−0.038(3)	0.247(5)
(7, 7)	−0.024(3)	0.15(1)

counting reasoning.

6. Conclusion

Heavy quarkonium states provide the opportunity to study interquark forces in QCD especially at large quark separations. This is due to the possibility to adopt a non-relativistic approach and to describe the interactions by means of a potential. Phenomenologically, the experimental data are well reproduced by 1 gluon exchange at small quark-antiquark separations and by a linear potential at large distances. Fine and hyperfine splittings are naturally explained by a long-range part of the forces of predominantly scalar Lorentz structure.

A full understanding of interquark forces requires a comprehensive non-perturbative treatment of QCD. As such, lattice gauge theory offers the most promising prospects. The most precise lattice results to date originate from investigations in the quenched approximation. Here systematic effects due to finite lattice spacing are becoming the main source of uncertainty and should be studied further. Simulations in full QCD have reached a quality which permits more than qualitative statements. Yet, as far as the interquark potential is concerned, especially larger lattices are a must for future improvements. This does not present any principle obstacle but will require vaster computer resources than presently available.

Nevertheless, as of today it can be safely concluded that lattice investigations provide convincing numerical evidence for the confinement hypothesis. The results for the interquark potential show a Coulomb behavior at small distances and a linear rise at large quark separations, both in quenched QCD and in the full theory for distances up to 1 fm. Determinations of the spin dependent potential favor scalar confinement quite clearly. Measurements of gluon and quark field distributions between a heavy $Q\overline{Q}$ pair support the Nielsen-Olesen conjecture of color-electric confinement and suggest a trend towards realization of a perturbative vacuum inside the flux tube. Forces between non-fundamental representations which may be important to understand nuclear systems indicate genuine non-perturbative effects.

Acknowledgements

It is a pleasure to thank the organizers of the workshop for the opportunity to obtain a comprehensive overview of all the challenges laid out by QCD, as well as the achievements in 20 years of working on QCD. Part of the material could not have been presented here without the help of my co-workers from the MT_c group. G. Bali and K. Schilling are thanked for letting me use their data prior to publication. While preparing this review I enjoyed discussions with J. Fingberg, L. Kärkkäinen, H. Markum, C. Michael, B. Petersson and G. Schierholz and benefitted from assistance by G. Eickmeyer, J. Engels and P. Lacock. This piece of work has been supported by the DFG under contract number PE-340/3-1.

References

1. W. Buchmüller and S. Cooper, in *High Energy Electron-Positron Physics*, ed. A. Ali and P. Söding (World Scientific, Singapore, 1988).
2. J. H. Kühn and P. M. Zerwas, *Phys. Rep.* **167** (1988) 321.
3. D. Gromes, W. Lucha and F. F. Schöberl, *Phys. Rep.* **200** (1991) 127.
4. J. J. Aubert et al., *Phys. Rev. Lett.* **33** (1974) 1406;
   G. S. Abrams et al., *Phys. Rev. Lett.* **33** (1974) 1453.
5. T. Appelquist and H. D. Politzer, *Phys. Rev. Lett.* **34** (1975) 43.
6. E. Eichten et al., *Phys. Rev. Lett.* **34** (1975) 369.
7. J. L. Richardson, *Phys. Lett.* **B82** (1979) 272.
8. W. Fischler, *Nucl. Phys.* **B129** (1977) 157;
   A. Billoire, *Phys. Lett.* **B92** (1980) 343.
9. C. Quigg and J. Rosner, *Phys. Lett.* **B71** (1977) 153.
10. A. Martin, *Phys. Lett.* **B93** (1980) 338.
11. C. Quigg and J. Rosner, *Phys. Rev.* **D23** (1981) 2625.
12. M. B. Voloshin, *Nucl. Phys.* **B154** (1979) 365;
    H. Leutwyler, *Phys. Lett.* **B98** (1981) 447.
13. H. G. Dosch and U. Marquard, *Phys. Rev.* **D35** (1987) 2238.
14. K. Igi and S. Ono, *Phys. Rev.* **D33** (1986) 3349.
15. K. Wilson, *Phys. Rev.* **D10** (1974) 2445.
16. F. J. Wegner, *J. Math. Phys.* **12** (1971) 2259.
17. H. J. Rothe, *Lattice Gauge Theories – An Introduction* (World Scientific, Singapore, 1992).
18. K. Symanzik, *Nucl. Phys.* **B226** (1983) 187, 205.
19. R. Kenway, these proceedings.
20. M. Lüscher, R. Narayanan, P. Weisz and U. Wolff, preprint DESY 92-025.
21. M. Creutz, *Phys. Rev.* **D21** (1980) 2308.
22. C. Lang and C. Rebbi, *Phys. Lett.* **B115** (1982) 137.

23. E. Kovacs, *Phys. Rev.* **D25** (1982) 871, 3312;
J. D. Stack, *Phys. Rev.* **D27** (1983) 412, **D29** (1984) 1213;
S. W. Otto and J. D. Stack, *Phys. Rev. Lett* **52** (1984) 2328;
D. Barkai, K. Moriarty and C. Rebbi, *Phys. Rev.* **D30** (1984) 1293, 2201;
K. C. Bowler et al., *Phys. Lett.* **B163** (1984) 367;
A. Hasenfratz et al., *Z. Phys.* **C25** (1984) 191;
R. Sommer and K. Schilling, *Z. Phys.* **C29** (1985) 95;
S. Itoh, Y. Iwasaki and T. Yoshie, *Phys. Rev.* **D33** (1986) 1806;
J. Flower and S. W. Otto, *Phys. Rev.* **D34** (1986) 1649;
F. Gutbrod, *Phys. Lett.* **B186** (1987) 389; *Z. Phys.* **C37** (1987) 143;
N. A. Campbell, A. Huntley and C. Michael, *Nucl. Phys.* **B306** (1988) 51;
H.-Q. Ding, *Phys. Lett.* **B200** (1988) 133;
C. Michael and M. Teper, *Nucl. Phys.* **B314** (1989) 347;
S. J. Perantonis, A. Huntley and C. Michael, *Nucl. Phys.* **B326** (1989) 544;
S. J. Perantonis and C. Michael, *Nucl. Phys.* **B347** (1990) 854;
S. J. Perantonis and C. Michael, preprint LTH-261; LTH-262.
24. A. Huntley and C. Michael, *Nucl. Phys.* **B270** (1986) 123.
25. I. J. Ford, R. H. Dalitz and J. Hoek, *Phys. Lett.* **B208** (1988) 286.
26. R. Sommer, *Nucl. Phys.* **B306** (1988) 180.
27. H.-Q. Ding, C. F. Baillie and G. C. Fox, *Phys. Rev.* **D41** (1990) 2912;
H.-Q. Ding, *Phys. Rev.* **D42** (1990) 2350; **D44** (1991) 2200.
28. G. Bali and K. Schilling, preprints WUB-92-02, WUB-92-29.
29. S. Booth et al. (UKQCD Collaboration), preprint LTH-285.
30. S. Booth et al. (UKQCD Collaboration), *Phys. Lett.* **B275** (1992) 424, preprint LTH-284.
31. H. Joos and I. Montvay, *Nucl. Phys.* **B225** (1983) 565;
E. Laermann et al., *Phys. Lett.* **B173** (1986) 437;
M. Campostrini et al., *Phys. Lett.* **B193** (1987) 78;
K. D. Born et al., *Phys. Rev.* **D40** (1989) 1653.
32. K. D. Born et al. (*MT*$_c$ Collaboration), *Nucl. Phys.* B *(Proc. Suppl.)* **20** (1991) 394 and in preparation.
33. M. Teper, *Phys. Lett.* **B183** (1986) 345; **B185** (1987) 121;
M. Albanese et al. (APE Collaboration), *Phys. Lett.* **B192** (1987) 163.
34. C. Michael and S. Perantonis, *Nucl. Phys.* B *(Proc. Suppl.)* **20** (1991) 177.
35. M. Gao, *Nucl. Phys.* B *(Proc. Suppl.)* **20** (1991) 185.
36. M. Lüscher, K. Symanzik and P. Weisz, *Nucl. Phys.* **B173** (1980) 365;
M. Lüscher, *Nucl. Phys.* **B180** (1981) 317.
37. P. Lepage and P. Mackenzie *Nucl. Phys.* B *(Proc. Suppl.)* **20** (1991) 173.
38. C. Michael, *Phys. Lett.* **B283** (1992) 103.
39. M. Lüscher, R. Sommer, P. Weisz and U. Wolff, preprint DESY 92-096;
J. Fingberg, U. Heller and F. Karsch, preprint BI-TP 92-26;
A. X. El-Khadra et al., preprint FERMILAB-PUB-91/354-T.
40. E. Eichten and F. Feinberg, *Phys. Rev.* **D23** (1981) 2724.
41. D. Gromes, *Z. Phys.* **C26** (1984) 401.
42. S. N. Gupta, S. F. Radford and W. W. Repko, *Phys. Rev.* **D26** (1982) 3305.
43. J. Pantaleone, Y. J. Ng and S.-H. H. Tye, *Phys. Rev.* **D33** (1986) 777.
44. V. S. Dotsenko and S. N. Vergeles, *Nucl. Phys.* **B169** (1980) 527.
45. A. Huntley and C. Michael, *Nucl. Phys.* **B286** (1987) 211.
46. M. Campostrini, *Nucl. Phys.* **B256** (1985) 717.
47. C. Michael, *Phys. Rev. Lett.* **56** (1986) 1219.
48. C. Michael and P. E. L. Rakow, *Nucl. Phys.* **B256** (1985) 640;
P. de Forcrand and J. D. Stack, *Phys. Rev. Lett.* **55** (1985) 1254;
M. Campostrini, K. Moriarty and C. Rebbi, *Phys. Rev. Lett.* **57** (1986) 44;
I. J. Ford, *J. Phys.* **G15** (1989) 1571.
49. Y. Koike, *Nucl. Phys.* **B216** (1989) 184.
50. E. Laermann et al. (*MT*$_c$ Collaboration), *Nucl. Phys.* B *(Proc. Suppl.)* **26** (1992) 268; K. D. Born et al. (*MT*$_c$ Collaboration), in preparation.
51. H. B. Nielsen and P. Olesen, *Nucl. Phys.* **B61** (1973) 45.
52. O. Alvarez, *Phys. Rev.* **D24** (1981) 440.
53. J. F. Donoghue and C. De Tar, *Annu. Rev. Nucl. Sci.* **33** (1983) 235.
54. J. Ambjørn, P. Olesen and C. Peterson, *Nucl. Phys.* **B244** (1984) 262;
C. Peterson and L. Sköld, *Nucl. Phys.* **B255** (1985) 365;
M. Flensburg and C. Peterson, *Phys. Lett.* **B153** (1985) 412.
55. M. Fukugita and I. Niuya, *Phys. Lett.* **B132** (1983) 374.
56. J. Flower and S. Otto, *Phys. Lett.* **B160** (1985) 128.
57. R. Sommer, *Nucl. Phys.* **B291** (1987) 673.
58. R. W. Haymaker and J. Wosiek, *Acta Phys. Polon.* **B21** (1990) 403;
Phys. Rev. **D43** (1991) 2676.
59. M. Lüscher, G. Münster and P. Weisz, *Nucl. Phys.* **B180** (1981) 1.
60. C. Michael, *Nucl. Phys.* **B280** (1987) 13.
61. W. Feilmaier, M. Faber and H. Markum, *Phys. Lett.* **B221** (1989) 363;
Phys. Rev. **D39** (1989) 1409;
M. Müller et al., *Nucl. Phys.* **B335** (1990) 502;
W. Sakuler et al., *Phys. Lett.* **B276** (1992) 155.
62. E. Laermann, P. Schildberg and P. M. Zerwas, in preparation.
63. R. Altmeyer et al. (*MT*$_c$ Collaboration), preprint HLRZ 92-17.
64. C. Bernard, *Phys. Lett.* **B108** (1982) 431; *Nucl. Phys.* **B219** (1983) 341;
J. Ambjørn, P. Olesen and C. Peterson, *Nucl. Phys.* **B240** (1984) 189;
C. Michael, *Nucl. Phys.* **B259** (1985) 58;
L. A. Griffiths, C. Michael and P. Rakow, *Phys. Lett.* **B150** (1985) 196;
N. A. Campbell, I. H. Jorysz and C. Michael, *Phys. Lett.* **B167** (1986) 91.
65. C. Michael, *Nucl. Phys.* B *(Proc. Suppl.)* **26** (1992) 417.
66. I. H. Jorysz and C. Michael, *Nucl. Phys.* **B302** (1987) 448.
67. H. Markum et al., *Phys. Rev.* **D31** (1985) 2029;
S. Ohta, M. Fukugita and A. Ukawa, *Phys. Lett.* **B173** (1986) 15.
68. A. M. Green, C. Michael and J. Paton, *Phys. Lett.* **B280** (1992) 11; preprint HU-TFT-92-12.